0029-3865

CBPF-NF-006/85

A PHENOMENOLOGICAL APPROACH TO ANGULAR MOMENTUM TRANSFER IN DEEP INELASTIC HEAVY ION COLLISIONS

by

V.C. Barbosa[2], P.C. Soares[2], E.C. Oliveira[1] and L.C. Gomes[1]

[1]Centro Brasileiro de Pesquisas Físicas - CNPq/CBPF
Rua Dr. Xavier Sigaud, 150
22290 - Rio de Janeiro, RJ - Brasil

[2]Instituto de Física
Universidade Federal do Rio de Janeiro
21910 - Rio de Janeiro, RJ - Brasil

ABSTRACT

The total angular momentum transfer measured in the reactions ^{165}Ho on ^{176}Yb, ^{154}Sm and ^{Nat}Ag at 1400 MeV and $^{86}Kr + ^{152}Sm$ at 610 MeV were analised on the basis of a classical model with friction forces including,besides the relative motion of the ions, their rotations and quadrupole vibrations. The ratios of tangential or pivotal to radial friction were fixed by the analysis and found to be 1/20. No strong evidences of the sticking mechanisms were found.

Key-words: Deep inelastic heavy ion reaction.

1 - INTRODUCTION

Since the interpretation made by Wilczynski [1] of orbiting phenomena in deep inelastic heavy ion collisions, classical descriptions of these reactions have been used to account for their main features. Here, following this trend in the literature, we analyse with a classical model the angular momentum transfer data of Pacheco et al. [2] for the reactions induced by ^{165}Ho on ^{176}Yb, ^{154}Sm and ^{Nat}Ag at 1400 MeV in the laboratory frame of reference as well as the data of Christensen et al. [3] for the $^{86}Kr + ^{152}Sm$ reaction at $E_{Lab} = 610$ MeV.

In our model the collective degrees of freedom are the relative motion of the centers of masses of the ions, their intrinsic rotations and the quadrupole vibrations, the latter taken in an approximated way. The nuclear force we used is the proximity potential as derived in [4] without any adjustable parameter. For the friction forces we took the proximity formula given by Randrup [5] but we considered the strenghts of the radial and tengential functions as adjustable parameters. We further introduced a pivotal friction taken to be proporcional to the radial friction with its strenght treated also as an adjustable parameter. In this way we could obtain in a single model the sliding, rolling and sticking mechanisms for the angular momentum transfer by simply varying the strenghts of the tangential and pivotal frictions.

We assumed that the vibrational degrees of freedom only couple to the relative radial motion of the ions and therefore

do not interfere with the angular momentum transfer mechanism. The contribution of vibrations to the energy loss has been taken into consideration by a simple procedure derived from the results of Gross et al.[6].

2 - THE EQUATION OF MOTION

We assume the following Lagrangean:

$$L = \frac{1}{2}\mu(\dot{r}^2+r^2\dot{\theta}^2) + \frac{1}{2}I_1w_1^2 + \frac{1}{2}I_2w_2^2 - V_c(r) - V_N(r) \qquad (2.1)$$

where μ is the reduced mass of the system and I_1, I_2 are the moments of inertia of the two ions calculated as in a uniform spherical mass distribution:

$$I = \frac{2}{5}MR^2$$

with

$$R = 1.28\,A^{1/3} - 0.76 + 0.8\,A^{-1/3},$$

the equivalent nuclear radius[4]. The variables r and θ are the polar coordinates for the relative motion of the centers of masses for the two ions.

Note that the Lagrangean given by eq. (2.1) describes the relative motion of the two ions assumed to be frozen spheres subject to the electrostatic $V_c(r)$ and nuclear $V_N(r)$ interactions. The rotation of the ions is allowed by introducing their angular

velocities w_1 and w_2 in eq. (2.1). The possibility of vibrations of the ions is not included in eq. (2.1) but we will take them into consideration by a simple treatment to be described in next section.

For the eletrostatic interaction we took the coulomb field corrected for the finite size of the ions.

$$V_c(r) = \begin{cases} \dfrac{Z_1 Z_2 e^2}{r} & \text{for} \quad r > R_c \\ \dfrac{Z_1 Z_2\, e^2 (3R_c^2 - r^2)}{2R_c^3} & \text{for} \quad r < R_c \end{cases}$$

where

$$R_c = 1.3\ (A_1^{1/3} + A_1^{1/3}) \quad \text{fm}$$

For the nuclear potential $V_N(r)$ we used the proximity formula of Blocki et al. [4]:

$$V_N(r) = 4\pi\gamma\bar{c}\ b\ \Phi_0\ \left(\frac{r - c_1 - c_2}{b}\right)$$

with

$$b = 1 \text{ fm}$$

$$\gamma = 1 \text{ MeV fm}^{-2}$$

$$\bar{c} = c_1 c_2/(c_1 + c_2)$$

where c_1, c_2 are the half density radius of the ions:

$$c = \left(1 - \left(\frac{b}{R}\right)^2\right) R .$$

The friction forces are obtained from the following

Rayleigh's function:

$$F = \frac{1}{2}\,\beta\,\Gamma(r)\left[\dot{r}^2 + \alpha_1 r^2\left(\dot{\theta} - \frac{R_1 w_1}{R_1+R_2} - \frac{R_2 w_2}{R_1+R_2}\right)^2 + \alpha_2 \bar{c}^2 (w_1-w_2)^2\right] \quad (2.2)$$

The parameters β, α_1 and α_2 were introduced in eq. (2.2) to allow the adjustments of the strenghts of the different friction coefficients. Thus, β permits the adjustment of the radial friction strenght while α_1 and α_2 permit the adjustments of the tangential and pivotal friction strenghts respectively. $\Gamma(r)$ plays the role of the radial form factor for the frictions and is given by the one-body friction proximity formula of Randrup [5]:

$$\Gamma(r) = 4\pi\,\eta_0\,\bar{c}\,\phi_0\left(\frac{r-c_1-c_2}{b}\right)$$

with

$$\eta_0 = 2.63 \times 10^{-23}\ \text{MeV s/fm}^{-4}$$

Let us observe now that setting $\beta = 1$, $\alpha_1 = 0.5$ and $\alpha_2 = 0$ the friction forces derived from eq. (2.2) are the same as those used by Blocki et al. [4] in the simulation of $^{86}Kr + {}^{197}Au$ therein.

From eqs. (2.1) and (2.2) one can easily obtain the equations of motion:

$$\mu(\ddot{r} - r\dot{\theta}^2) = -\frac{d}{dr}\,(V_c(r) + V_N(r)) - \beta\Gamma(r)\,\dot{r} \quad (2.3)$$

$$\frac{d}{dt}\,(\mu r^2\dot{\theta}) = -\frac{\beta\Gamma(r)\alpha_1 r^2}{R_1+R_2}\,((R_1+R_2)\dot{\theta} - R_1 w_1 - R_2 w_2) \quad (2.4)$$

$$\frac{d}{dt}(I_1 w_1) = \frac{\beta\alpha_1 \Gamma(r) r^2 R_1}{(R_1+R_2)^2}((R_1+R_2)\dot{\theta} - R_1 w_1 - R_2 w_2) - \beta\alpha_2 \bar{c}^2 \Gamma(r)(w_1-w_2) \tag{2.5}$$

$$\frac{d}{dt}(I_2 w_2) = \frac{\beta\alpha_1 \Gamma(r) r^2 R_2}{(R_1+R_2)^2}((R_1+R_2)\dot{\theta} - R_1 w_1 - R_2 w_2) + \beta\alpha_2 \bar{c}^2 \Gamma(r)(w_1-w_2) \tag{2.6}$$

From eqs. (2.4) to (2.6) we obtain the conservation of angular momentum:

$$L_0 = \mu r^2 \dot{\theta} + I_1 w_1 + I_2 w_2 \tag{2.7}$$

where L_0 is the initial angular momentum of the system.

The rate of energy dissipation is given by twice the Rayleigh's function and we have:

$$\frac{dE}{dt} = -2F \quad , \tag{2.8}$$

what shows that the system evolves during the collision in such a trajectory as to minimize F.

Let us now discuss from the point of view of eqs. (2.3) to (2.6) the rolling and sticking limits for the collisions.

Let us first assume the vanishing of the pivotal friction ($\alpha_2 = 0$). Then, from eqs. (2.5) and (2.6) we obtain the following first integral of motion:

$$\frac{I_2 w_2}{R_2} = \frac{I_1 w_1}{R_1} \quad , \tag{2.9}$$

and, from the minimization of F we get the asymptotic behaviour:

$$(R_1+R_2)\dot{\theta} = R_1w_1 + R_2w_2 \quad . \tag{2.10}$$

Now, eqs. (2.7), (2.9) and (2.10) permit to write w_1, w_2 and $\dot{\theta}$ as a function of r. In particular, for the total angular momentum transfered, J, we have

$$J \equiv I_1w_1 + I_2w_2 = (1 + \frac{5}{2}\,(\frac{r}{R_1+R_2})^2)^{-1}\, L_0 \tag{2.11}$$

If we further assume that during the dissipative process, the ions stay at a constant distance R_1+R_2 apart we get the well know result:

$$J = \frac{2}{7}\, L_0 \tag{2.12}$$

for the rolling limit which says that J is a fraction (2/7) of the inicial angular momentum L_0, independent of the system under consideration.

If now, α_1 and α_2 are both different from zero, the first integral of motion given by eq. (2.9) does not follow but instead, besides eq. (2.10), F predicts a new equation for the asymptotic motion:

$$w_1 = w_2 \quad . \tag{2.13}$$

Then, eqs. (2.10) and (2.13) give:

$$\dot{\theta} = w_1 = w_2 \tag{2.14}$$

the so called stricking limit, which together with eq. (2.7) give the following asymptotic value for the transferred total angular momentum:

$$J = (1 + \frac{\mu r^2}{I_1+I_2})^{-1} L_0 \quad . \qquad (2.15)$$

In the case of symmetric systems, $(I_1=I_2)$ and $\mu = \frac{1}{2} M_1 = \frac{1}{2} M_2$, eq. (2.15) reduces to eq. (2.11) and there is no possibility of distinguishing between the rolling and sticking mechanisms investigating only the angular momentum transfered.

3 - THE ^{40}AR + ^{232}TH SYSTEM

We considered the $^{40}Ar + ^{232}Th$ system to illustrate the results one may possibly obtain from the equations of motion of previous section for different values of the parameters α_1 and α_2. The reason for such a choice is twofold: first, the $^{40}Ar + ^{232}Th$ reaction was extensively studied by Gross and collaborators [6,7], using a classical model. Second, it is a very assymetric system, and therefore the rolling and sticking limits are very differentiated. The energy of the system was taken to be 379 MeV in the laboratory frame of reference.

Fig. 1 shows the results of simulations done with different values of α_1 and α_2. The horizontal axis is the initial angular momentum L_0 in units of $\hbar$ and the vertical one the values of J also in units of $\hbar$. The two straight lines labeled (1) and (2) correspond to the limit of eqs. (2.11) and (2.14) respectively, setting $r = R_1+R_2$. In all simulations we have set $\beta = 40$ which is our best fit based on the energy loss

versus angle in the Wilczynski diagram. We will discuss this point in more detail when we consider fig. 2. Curves (a), (b) and (c) were obtained by setting α_1 = 0.05, 1 and 5 respectively and α_2 = 0 in all of them. They correspond to the rolling mechanism.

The transfer of angular momentum occurs only for values of L_0 below the grazing value of 220 $\hbar$. It is more abrupt the larger the value of α_1 up to a maximum value and from then on it is limited by the asymptotic baheviour of the equations of motion as discussed in the previous section. The latter corresponds to the region between 155 $\hbar$ to 195 $\hbar$ for both curves (b) and (c). Observe that the fixed radial distance from where the ions roll one over the other is larger than R_1+R_2 as shown by the fact that both curves (b) and (c) are below the limit set by the straight line (1). In the case of curve (a) for which α_1 = 0.05 it is interesting to observe the very slow increase of J for decreasing values of L_0 and the lack of the asymptotic behaviour. This is a case we would consider as a misture of sliding and rolling mechanisms. Curves (d) and (e) correspond to $\alpha_1 = \alpha_2$ = 1.0 and 0.1 respectively. Curve (d) exhibits the characteristic asymptotic bahaviour of the sticking limit given by eq. (2.14) (for a value of r again larger than R_1+R_2) as expected from the large values of α_1 and α_2. Curve (e) is similar to curve (a) but with the inclusion of the pivotal friction. Though J takes values above the limit give by eq. (2.12) it does not show the asymptotic behaviour as given by eq. (2.14).

Fig. 2 exhibits the Wilczynski diagram for the reaction under consideration. The horizontal axis is the scattering angle in the C.M. in degrees and the horizontal one is the energy

in the C.M. for the inelastic channels. Curves (b) and (a) are the same as predicted by Gross et al.[6,7] with and without the vibrations of the ions, respectively. Curves (d) and (e) were obtained from our equations of motion of the previous section with the following parameters: $\beta = 1$; $\alpha_1 = 1/2$; $\alpha_2 = 0$ for curve (e) and $\beta = 40$; $\alpha_1 = \alpha_2 = 0.05$ for curve (d). Therefore curve (e) corresponds to the one-body friction of Randrup[5] and we may observe that this friction is rather insufficient to reproduce the large energy loss in the deep inelastic channels. Curve (d) compares very favourably with the curve (a) of Gross in the region of large inelasticity and it fixes the value of $\beta = 40$ that we will use throughout this paper. The disagreement between curves (a) and (d) near the grazing angle could be easily corrected if we had allowed ourselves to vary the proximity potentials. We did not consider important in what follows the difference of 3 degrees for the grazing angles between curves (a) and (d).

We will consider now the contribution of vibrations to the energy loss of the reaction. Let us assume that each ion is an elastic sphere which may vibrate in the quadrupole (isoescalar) vibration modes. Let us call y the coordinate of the point on the surface of one of the ions, with respect to its center of mass, closest to the surface of the other. We set:

$$\mu' \ddot{y} + \mu' \gamma \dot{y} + \mu' w_0^2 y = f$$

as the equation of motion for this point where μ' is the inertia associated with the quadrupole motion of the ion, w_0 is the quadrupole isoscalar giant ressonance frequency and γ is responsible for the internal dissipation of the vibrational energy.

f is the force produced by the other ion which, from our point of view, comes exclusively from the radial friction force. During the collision, the point of contact between the surfaces moves due to friction, forcing the excitation of the vibration. This forced motion is much slower than the natural vibration of the ions and we therefore make the somewhat oversimplified assumption of neglecting the $\ddot{y}$ and $\dot{y}$ terms in the last equation. Then, we get

$$y = \frac{f}{\mu' w_0^2} \quad .$$

The energy of vibration for each ion results to be:

$$E_{vib} = \frac{\mu'}{2} w_0^2 y^2 = \frac{1}{2} \frac{f^2}{\mu' w_0^2} \quad . \tag{3.1}$$

We further assume that f is approximately given by

$$|f| = \frac{|Q|}{\Delta} \tag{3.2}$$

where Q is the energy loss for the relative motion of the ions without including vibrations and Δ is a mean distance that the ions move when under the action of the radial friction force. Substituting eq. (3.2) into eq. (3.1) we finally arrive at

$$E_{vib} = \frac{Q^2}{2\mu' w_0^2 \Delta^2}$$

as the energy transfered to vibration for each ion.

Let us now observe that

$$\mu' = \eta A$$

and [8]

$$\hbar w_0 = \varepsilon A^{-1/3} \quad , \quad (\varepsilon = 64.7 \text{ MeV}) \quad .$$

Then, the total energy transfered to vibration of both ions is

$$E_{tot} = \frac{Q^2}{Q_0}$$

where

$$Q_0 = \delta \left(\frac{A_1^{1/3} A_2^{1/3}}{A_1^{1/3} + A_2^{1/3}} \right) \tag{3.3}$$

with

$$\delta = 2\eta \left(\frac{\varepsilon \Delta}{h} \right)^2 \quad . \tag{3.4}$$

The actual energy loss during the reaction including vibration is then:

$$|Q^*| = |Q| + \frac{Q^2}{Q_0} \quad . \tag{3.5}$$

It is interesting to observe that if we assume Δ to be constant eq. (3.3) tells us how Q_0 varies from one system to another depending only on the parameter δ. The value of this parameter can be estimate from the data of Gross et al.[6]. We found Q_0 = 200 MeV and δ = 91.03 MeV.

Curve (c) in Fig. 2 is the application of eq. (3.5) to the data corresponding to curve (a) of the same figure. Note the reasonable agreement between curve (b) calculated by Gross and curve (c) obtained from our estimate of the vibrational energy.

The values of η used is the (3/10) m value associated with the irrotational quadrupole vibration of the ion, where m

is the nucleon mass. Substituting these results into eq. (3.4) we obtain

$$\Delta = 1.23 \text{ fm}$$

which is a very reasonable value of Δ for these reactions.

4 - THE EXPERIMENTAL DATA FITTING

Pacheco et al.[2] measured the angular momentum transferred in reaction induced by ^{165}Ho on ^{176}Yb, ^{148}Sm and ^{Nat}Ag at $E_{Lab} = 1400$ MeV. We simulated these reactions using the equations of motion of section 2. We observe that in all of them, the angular momentum transferred is insensitive to the value of α_2. This can be understood as due to the fact that these systems are close to the symmetric situation which we have shown to be insensitive to the differentiation of the rolling and sticking mechanisms. Due to this we were enable to substantiate the conclusion in reference (2) that the experimental data clearly favours the sticking mechanism. As the parameters δ and β are fixed by the previous analysis of the $^{40}Ar + ^{232}Th$ reaction, we used the ^{165}Ho reaction to fix the parameter α_1 which determines the strenght of the tangential friction.

Fig. 3 summarizes our analysis: the horizontal axis is the $|Q|$ value for the reactions in MeV and the vertical one is the angular momentum transferred in units of $\hbar$. The circular, quadrangular and triangular points are the experimental data for

^{176}Yb, ^{148}Sm and ^{Nat}Ag targets respectively. The three curves (excluding curve (a)) were simulated using the value $\alpha_1 = 0.05$ which best adjust the experimental data. We must observe that we have taken $\beta = 40$ fixed previously by the $^{40}Ar + ^{232}Th$ reaction.

The $|Q|$ value was obtained from eq. (3.5) with Q_0 fixed by eq. (3.3) with the same value $\delta = 91.03$ MeV found in the previous section. Curve (a) of Fig. 3 corresponds to $\alpha_1 = 0.063$ which shows, when compared to curve (b), how sensitive are the results varying the parameter α_1.

We have also studied the angular momentum transferred in the reaction $^{86}Kr + ^{154}Sm$ at $E_{Lab} = 610$ MeV measured by Christensen et al.[3] . Fig. 4 shows on the same axis as Fig. 3 the experimental data of ^{86}Kr, ^{154}Sm (circular points) and the theoretical results (full curves) for different values of α_2. Even though the system is somewhat asymmetric, the influence of α_2 on the simulation is almost negligible. The other parameters are the same as already fixed by the ^{165}Ho induced reactions i.e.; $\beta = 40$, $\alpha_1 = 0.05$ and $\delta = 91.03$ MeV. The fitting is rather good for Q values up to 150 MeV. We were enable to reproduce the data for large values of Q as the system fuses for $|Q| > 150$ MeV.

5 - CONCLUSIONS

The first point we would like to emphasize is the fact that with only four parameters we were able to describe classicaly the total mean angular momentum transferred in four different

reactions as well as the Wilczynski diagram for the $^{40}Ar+^{132}Th$ system at E_{Lab} = 379 MeV. This fact points towards the validity of the proximity formulae we used, which takes care of the size variations correctly among such diversified systems. With confidence in the parameters found it came as a surprise to us the very small values of α_1 and α_2 which give a factor of 20 between the radial and tangential or pivotal frictions. This points to the fact that contrary to what is stated in the literature, the mechanism of angular momentum transfer contains a substantial mixture of sliding. To emphasize this fact, we present in Fig. 5 the prediction of total angular momentum transfer for the ^{40}Ar + ^{232}Th reaction at E_{Lab} = 379 MeV. The horizontal and vertical axis are the same as in Fig. 3. Curves (a) and (b) are the results from the rolling and sticking mechanism respectively. From what we found the correct prediction is curve (c) which shows a substantialy small transfer as compared wich curves (a) and (b). Also it does not exhibit the maximum characteristic of the asymptotic limit.

Our analysis of Pacheco et al. data did not corroborate their conclusion that the reactions there observed favour the sticking in detriment to the rolling mechanism. It ssems to us that the invalidity of their argument comes from the use of the asymptotic limit result with is not reached for most of the energy sub-channels of the reactions investigated.

As a final point we would like to emphasize the efficiency of our tretament of the vibrational energy loss specially when we compare its extreme simplicity with the great complexity that vibrational degress of freedom introduce in any classical analysis.

6 - ACKNOWLEDGEMENTS

We would like to thank prof. J. Lopes Neto for reading the manuscript.

FIGURE CAPTIONS

FIG. 1 - The results of simulation done with different values of α_1 and α_2 as indicated. The horizontal axis is the initial angular momentum in units of $\hbar$ and the vertical one is the value of J in the same units. The two straight lines labeled 1 and 2, correspond to the limits of eqs. (2.11) and (2.14), respectively setting $r = R_1+R_2$. In all the simulations we have set $\beta = 40$.

FIG. 2 - The Wilczynski diagram to the reaction $^{40}Ar + ^{232}Th$ at 379 MeV. The horizontal axis is the scattering angle in the C.M. in degrees and the horizontal one is the energy also in the C.M. for the inelastic channels. Curves (a) and (b) are the same as predicted by Gross et al.[6,7] without and with consideration of the vibrations of the ions respectively. Curves (d) and (e) were obtained from our equations of motion of section 2 with the following parameters: $\beta = 1$; $\alpha_1 = 1/2$; $\alpha_2 = 0$ for curve (e) and $\beta = 40$; $\alpha_1 = \alpha_2 = 0.05$ for curve (d). Curve (c) is the application of eq. (3.5) to the data corresponding to curve (a) of the same figure.

FIG. 3 - The total angular momentum transferred for the reactions indicated. The horizontal axis is the $|Q|$ values for the reactions in MeV and the vertical one is the angular momentum transferred in units of $\hbar$. The circular, quadrangular and triangular points are the experimental data for ^{176}Yb, ^{148}Sm and ^{Nat}Ag targets respectively. In all curves we used $\beta = 40$. For curve (a) we took $\alpha_1 = 0.063$ while for the other curves we used $\alpha_1 = 0.05$.

FIG. 4 - The total angular momentum transferred for the reaction $^{86}Kr + ^{154}Sm$ at 610 MeV. The horizontal and vertical axis are the same as Fig. 3. The circular points are the experimental data and the full curves are the theoretical results for two different values of α_2 as indicated.

FIG. 5 - The total angular momentum transferred predicted for the reaction $^{40}Ar + ^{232}Th$ at 379 MeV. The horizontal and vertical axis are the same as Fig. 3. Curves (a) and (b) are the predictions from the rolling and sticking mechanisms respectively. Curves (c) exhibits the correct prediction bases on our analysis.

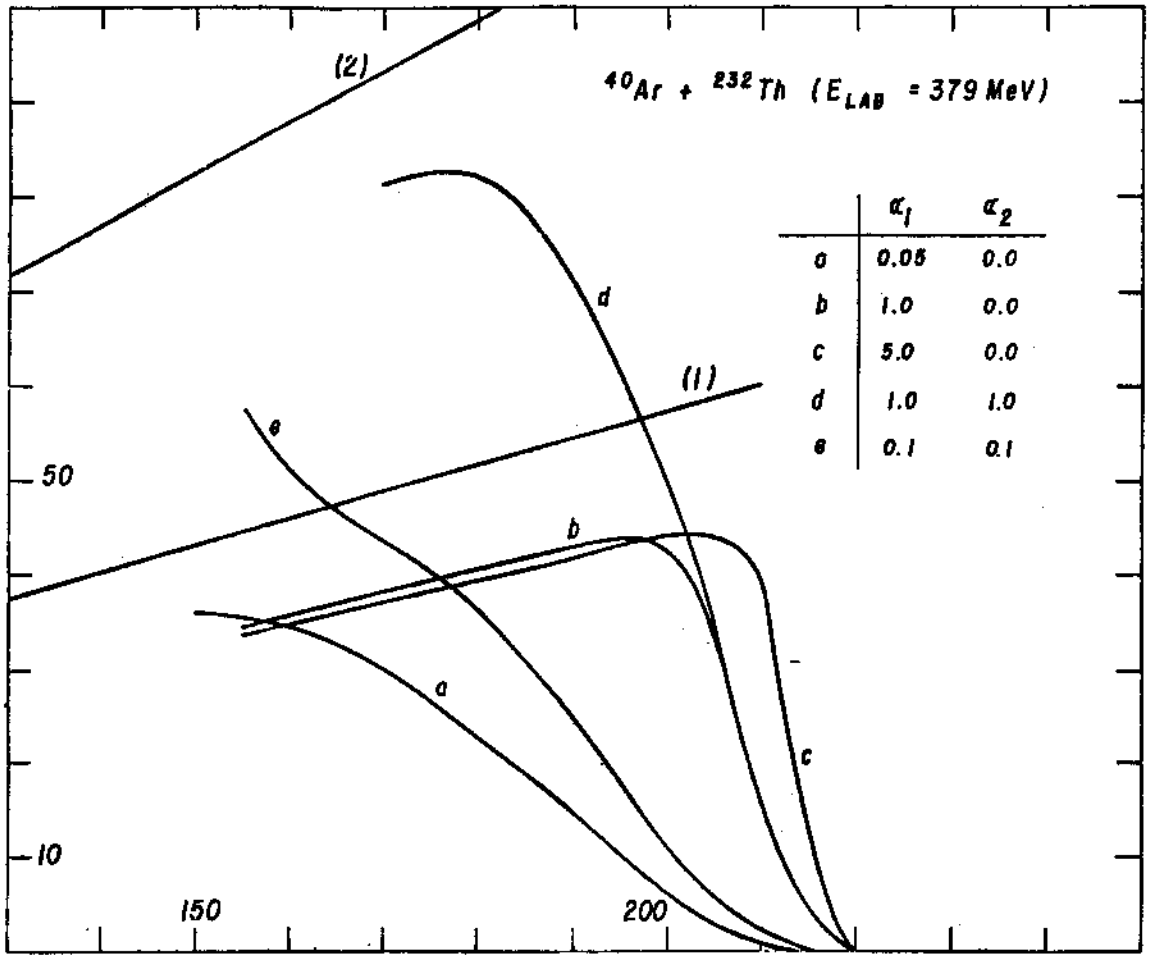

	α_1	α_2
a	0.05	0.0
b	1.0	0.0
c	5.0	0.0
d	1.0	1.0
e	0.1	0.1

Fig. 1

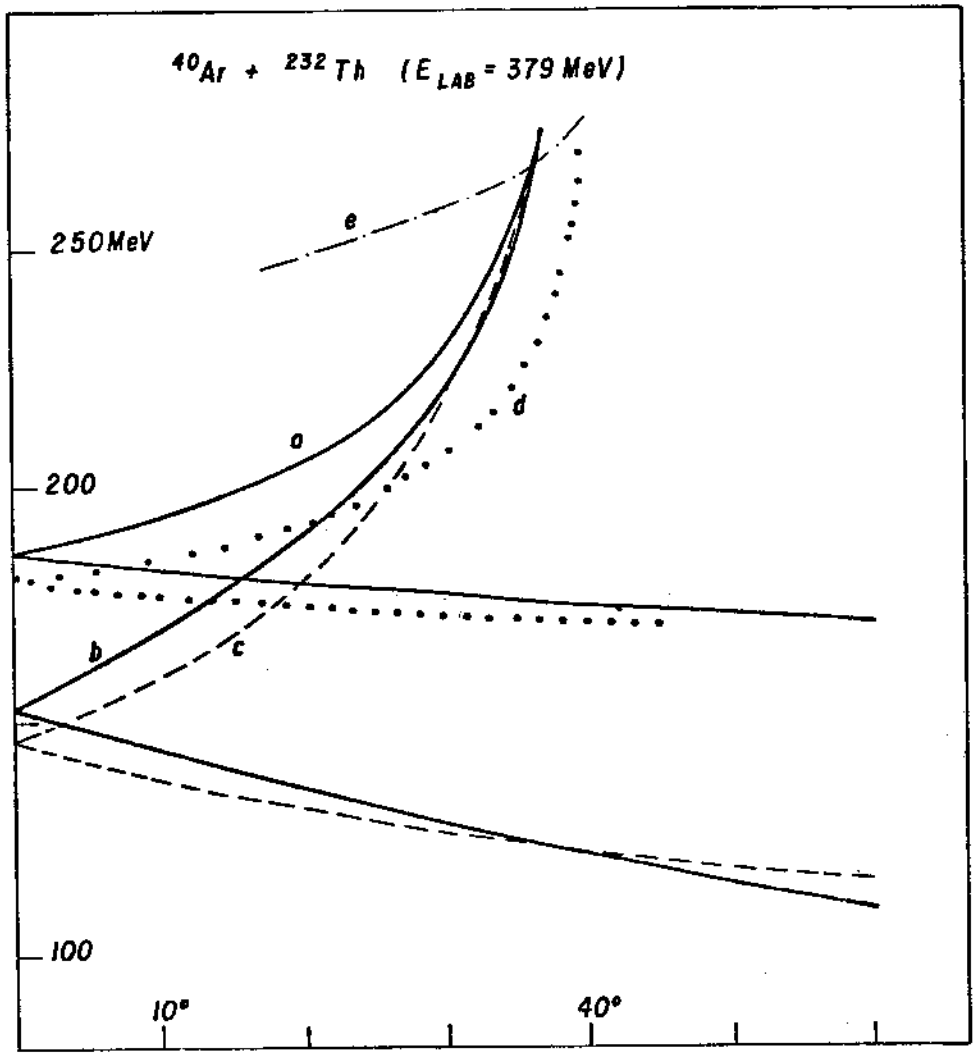

Fig. 2

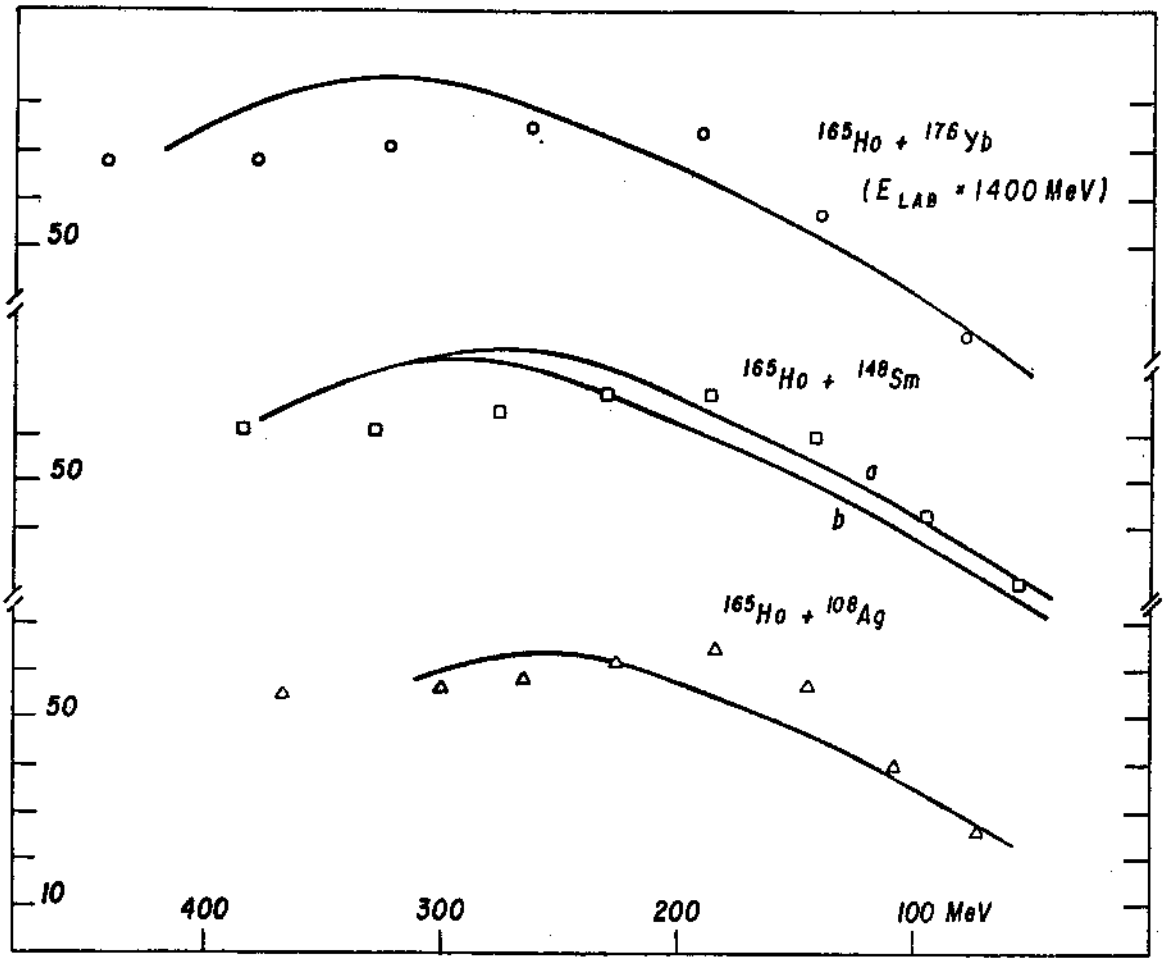
$^{165}Ho + ^{176}Yb$
(E_{LAB} = 1400 MeV)
$^{165}Ho + ^{148}Sm$
a
b
$^{165}Ho + ^{108}Ag$
50
50
50
10
400
300
200
100 MeV

Fig. 3

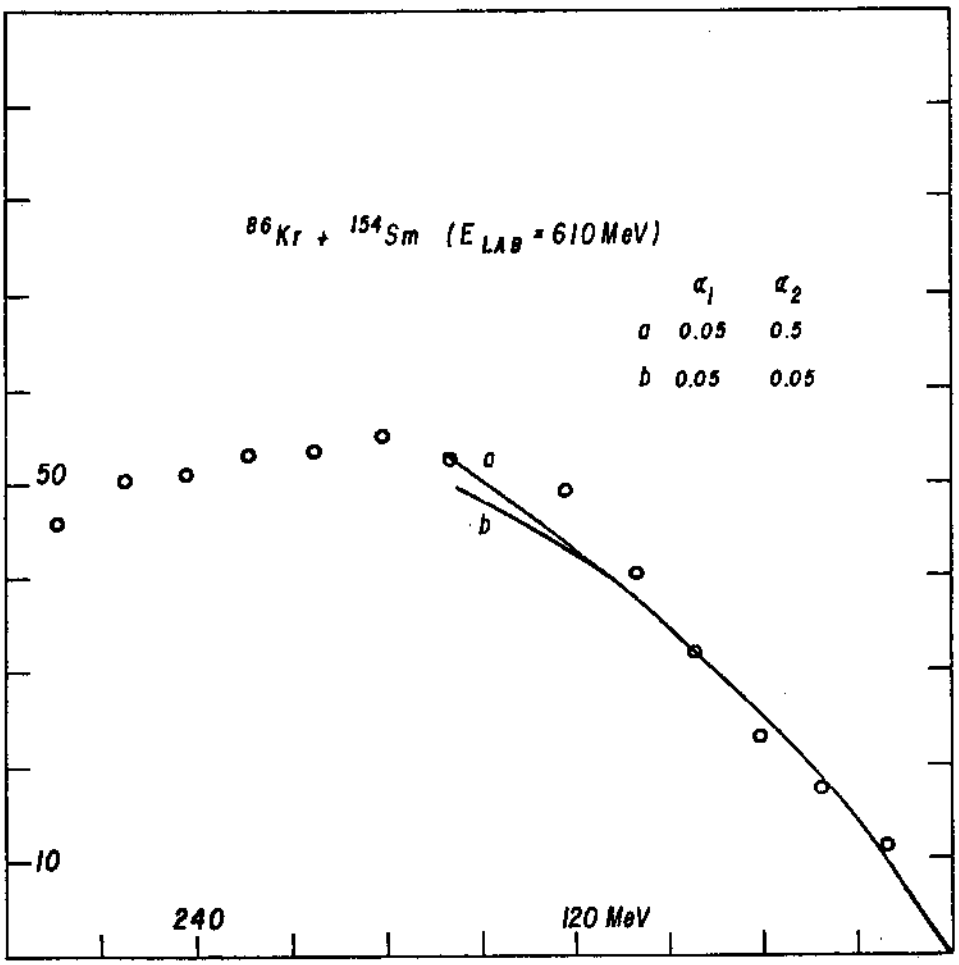
$^{86}Kr + ^{154}Sm$ (E_{LAB} = 610 MeV)
α_1 α_2
a 0.05 0.5
b 0.05 0.05
50
10
240
120 MeV
a
b

Fig. 4

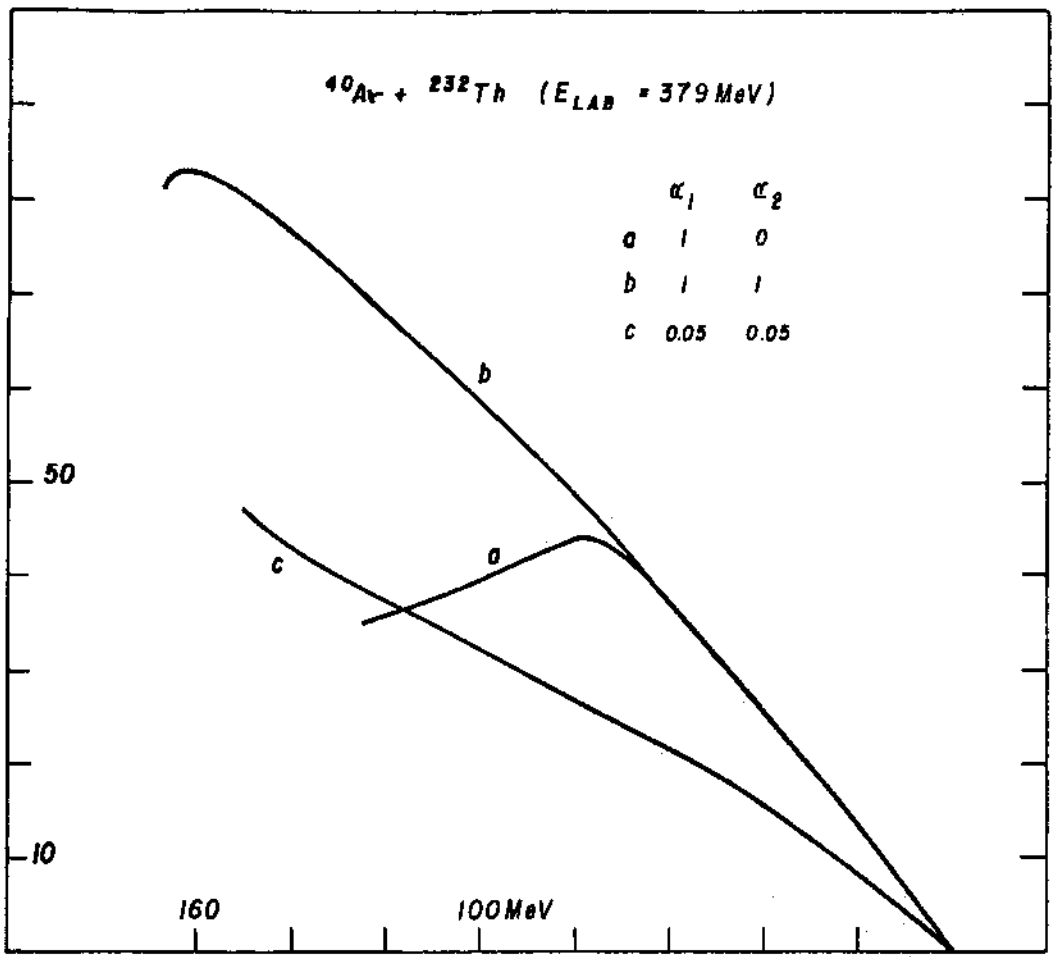
$^{40}Ar + ^{232}Th$ (E_{LAB} = 379 MeV)
α_1 α_2
a 1 0
b 1 1
c 0.05 0.05
b
a
c
50
10
160
100 MeV

Fig. 5

BIBLIOGRAPHY

1 - J. Wilczynski, Phys. Lett. 47B (1973) 484.

2 - A.J. Pacheco, G.J. Wozniak, R.J. MacDonald, R.M. Diamond, C.C. Hsu, L.G. Moretto, D.J. Morrisey, L.G. Sobotka, F.S. Stephens, Nucl. Phys. A397 (1983) 313.

3 - P.H. Christensen, Ole Hansen, O. Nathan, F. Videbaer, H. Freiesleben, H.C. Britt, S.Y. Van der Werf, Nucl. Phys., A390 (1982) 1336.

4 - J. Blocki, J. Randrup, W.J. Swiatecki, C.F. Tsang, Ann.Phys. (N.Y.) 105 (1977) 427.

5 - J. Randrup, Ann. Phys. (N.Y.) 112 (1978) 356.

6 - D.H.E. Gross, R.C. Nayak, L. Satpathy, Z. Phys. A299(1981)63.

7 - D.H.E. Gross, H. Kalinowski, Phys. Rep. 45 (1978) 175.

8 - F.E. Bertrand, Nucl. Phys., Ann. Rev. Nucl. Sci. 26(1976)457.